

## STUDY ON Mg-Al HYDROTALCITES IN FLAME-RETARDANT PAPER PREPARATION

Songlin Wang,\* Jianlin Huang, and Fushan Chen

Mg-Al-CO<sub>3</sub> LDH was synthesized, using co-precipitation, and was used in flame-retardant paper as filler. The crystallizations, granularities of Mg-Al LDH, and characters of flame-retardant papers were investigated through XRD, FT-IR, TEM, TG-DTA, and SEM techniques. The results indicated that Mg-Al hydrotalcites were layered hexagonal nanoparticles, with high positive charge density, perfectly crystallized structure, and striking performance in furnish retention improvement. Mg-Al hydrotalcites with high whiteness can improve the whiteness of flame-retardant paper; the whiteness of flame-retardant paper increased by 82.1% while the dosage of LDH was 20wt%, but the Mg-Al hydrotalcites affected the strength index of flame-retardant paper adversely. The flame-retardant papers based on fiber using Mg-Al hydrotalcites as fillers showed excellent flaming retarding performance. The oxygen index of the flame-retardant paper produced was above 25% at the dosage of 20wt%.

*Keywords: Mg-Al hydrotalcites; Flame-retardant paper; Flame retardant*

*Contact information: College of Chemical Engineering, Qingdao University of Science and Technology, Qingdao, Shandong Province, 266042. P. R. China;*

*\*Corresponding author: wangsongl@126.com*

### INTRODUCTION

Paper plays an important role in people's lives and social development, and it has a wide range of applications. However, typical paper and paper products are highly flammable. The burning of paper and paper products can contribute greatly to the seriousness of fires, so there is a strong motivation for development of flame-retardant treatments for paper (Guo 2006). There are mainly two types of flame-resistant paper. One category of the papers is composed of a combination of inorganic mineral fibers and natural fibers, where the former is the main ingredient. The inorganic fibers can include asbestos, mineral wool, glass fiber, and sepiolite fibers. The other class of paper with flame-retardant effect is made by adding a variety of flame-retardants in the pulp, or by dip-coating.

There are a wide range of flame-retardants that can be classified as reactive flame-retardants and added flame-retardants according to whether a chemical reaction is involved in polymer materials. Added flame retardant can also be divided into inorganic flame-retardants and organic flame-retardants (Abbott and Chalabi 1975; Routley 1975). The main types of inorganic flame retardants include metal hydroxides, metal oxides and alkali metal salts, ammonium salts, and molybdenum compounds. Organic flame-retardants include halogen flame-retardants, phosphorus flame-retardants, nitrogen flame-

retardants, and so on. One of the forefronts of current research in this area is to study and develop efficient, non-toxic, low-smoke, and cost-effective agents suitable for industrial production of inorganic halogen-free flame-retardants.

Layered double hydroxides (LDHs), also known as anionic clays, are a family of layered materials. Mg-Al- $\text{CO}_3$  LDH are well-known examples (Cavani et al. 1991). Mg-Al hydrotalcites are a type of flame retardant in smoke suppressor and filling functions. They can be described as efficient, halogen-free, non-toxic, and low-smoke flame retardants. The material exhibits advantages associated with both aluminum hydroxide and magnesium hydroxide flame retardants, and it also overcomes their respective deficiencies (Ren et al 2003; Xu et al 1990). The industrial production and application of Mg-Al hydrotalcites flame-retardants have been of interest both at home and abroad. In this study, Mg-Al hydrotalcites were prepared using the co-precipitation method, and were used in the flame-retardant paper as filler, the nature of hydrotalcites crystalline, and the flame-retardant properties of paper were studied.

## EXPERIMENTAL

### Materials

Softwood pulp was taken from a paper mill in Shandong province, China. The moisture content was 79.95wt%, and the beating degree was 33.8°SR. All chemicals were of analytical grade. The water used in the preparation and washing processes was deionized water. Polyacrylamide was purchased from Ciba Corporation, with a molecular weight of 5 million.

### Synthesis of Mg-Al Hydrotalcites

Mg-Al hydrotalcites were prepared using the co-precipitation method with separate nucleation and aging steps. To prepare the mixed salt solution (A), Mg  $(\text{NO}_3)_2 \cdot 6\text{H}_2\text{O}$  Al  $(\text{NO}_3)_3 \cdot 9\text{H}_2\text{O}$  was dissolved in deionized water with a fixed total ionic concentration of 0.5 mol/L and the Mg/Al molar ratio of 3:1. To prepare the mixed alkali solution (B), the required amounts of NaOH and  $\text{Na}_2\text{CO}_3$  were dissolved in deionized water. Then the salt solution (A) was added to the solution (B), slowly. The precipitate was stirred briskly for an hour, aged for 2 hours with slow stirring, and then aged for 48 hours. The white slurry was peptized 5 hours at 80°C. Then the product was washed and dried in a vacuum oven (Shi et al. 2005).

### Preparation of Flame-Retardant Paper

The pulp was separated into fibers in the fluffer with 30,000 revolutions according to the concentration of 1.5wt%, then solid hydrotalcites were added from 0 to 25% by mass, and the pulp was diluted to 0.5%. The dosage of CPAM was 0.03%. The paper was made on a sheet former at a target basis weight of 70 g/m<sup>2</sup>.

### Elemental Analysis and Essential Nature

The JSM-6700F EDS test was used to determine the elemental content of hydrotalcite colloidal samples. The particle size distribution was measured using a

Malvern Mastersizer 2000 laser particle size device (United Kingdom). Zeta potential was measured using ZetaPALS/90plus Zeta Potential Analyzer. A PCD-03 particle charge detector was used to measure charge demand.

#### **FT-IR Analysis of the Mg-Al Hydrotalcites**

A BRUKER VERTEX70 IR instrument was used to analyze the sample of Mg-Al hydrotalcites in terms of the presence of functional groups.

#### **X-ray Diffraction Analysis of Mg-Al Hydrotalcites**

XRD patterns were recorded on a D/MAX-RB X-ray diffractometer using a Cu target radiation ( $\lambda=0.15406$  nm) at 40 KV with a tube current of 100 mA and scan rate of  $8^\circ/\text{min}$ .

#### **TEM Analysis of Mg-Al Hydrotalcites Colloid**

The Mg-Al hydrotalcites colloids were diluted with deionized water several times; then the sample was observed with a Hitachi model H-800 transmission electron microscope to obtain their morphologies.

#### **SEM Analysis of Mg-Al Hydrotalcites and Flame-Retardant Paper**

The Mg-Al hydrotalcites and flame-retardant paper were observed with a JSM-6700F scanning electronic microscope. The samples were coated with gold before observation.

#### **TG-DTA Analysis of Mg-Al Hydrotalcites**

TG-DTA analysis was performed on a STA449 TGA thermogravimetric analyzer. The samples were heated from room temperature to  $800^\circ\text{C}$  at a heating rate of  $10^\circ\text{C}\cdot\text{min}^{-1}$  and under a nitrogen flow rate of  $20\text{ mL}\cdot\text{min}^{-1}$ . Samples of about 2 mg were used.

#### **Detection of the Physical Properties of Flame-Retardant Paper**

Tensile index, burst index, and whiteness were detected according to the relevant national standards.

#### **Detection of Oxygen Index of Flame-Retardant Paper**

The oxygen index of flame-retardant paper was measured using a LFY2606 oxygen index instrument. The paper was wetted for 24 hours and was cut into  $120\text{ mm} \times 13\text{ mm}$ , and then the sample was wetted for 4 hours again. The gas used was industrial grade, according to the GB3863 and GB3864 standards.

## **RESULTS AND DISCUSSION**

### **The Chemical Formula and Property of Hydrotalcites**

Tests with the JSM-6700F EDS device gave the content of each element. Its chemical formula, zeta potential, average particle size, and charge density are shown in Table 1.

The charged character and the particles sizes of the Mg-Al hydrotalcites colloidal particles can affect their application performance directly. The average size of a hydrotalcites particle is 118 nm in normal distribution. Hydrotalcite is added in the flame-retardant paper as a filler in the papermaking process. The electric potential of the particle can affect its retention greatly. Mg-Al hydrotalcites with high positive charge can be adsorbed in the fiber by the electrostatic charge neutralization in the process of papermaking. Such micro-flocculation not only improves the retention rate of the hydrotalcites, but also improves the retention of the fines; it is of great significance to improve the uniformity and optical property of the paper. At the same time, the micro-flocculation of hydrotalcites and fines can also perform the function of a retention and drainage system.

**Table 1.** Chemical Formula of Mg-Al-CO<sub>3</sub> LDH Compound

| Chemical structural formula  | Zeta potential/ mv | Particle size/ nm | Charge density / meq·g <sup>-1</sup> |
|--|--------------------|-------------------|--------------------------------------|
| MgAl <sub>0.3843</sub> (OH) <sub>2.4401</sub> (CO <sub>3</sub> ) <sub>0.3564</sub> •0.7129H <sub>2</sub> O | 23.16              | 118               | 22.95                                |

### FT-IR Analysis of Hydrotalcites

The FT-IR pattern of Mg-Al-CO<sub>3</sub> LDH is shown in Fig. 1. The spectrum shows the typical absorption peaks of carbonate LDH. The intense broad absorption at 3468.84 cm<sup>-1</sup> is associated with hydroxyl stretching vibrations. The water bending vibration appears at 1633.91 cm<sup>-1</sup>. The sharp absorptions at 1377.69 cm<sup>-1</sup> can be assigned to the asymmetric stretch of CO<sub>3</sub><sup>2-</sup>. The absorption peaks at 426.13 cm<sup>-1</sup> can be assigned to O-M-O vibrations in the layers.

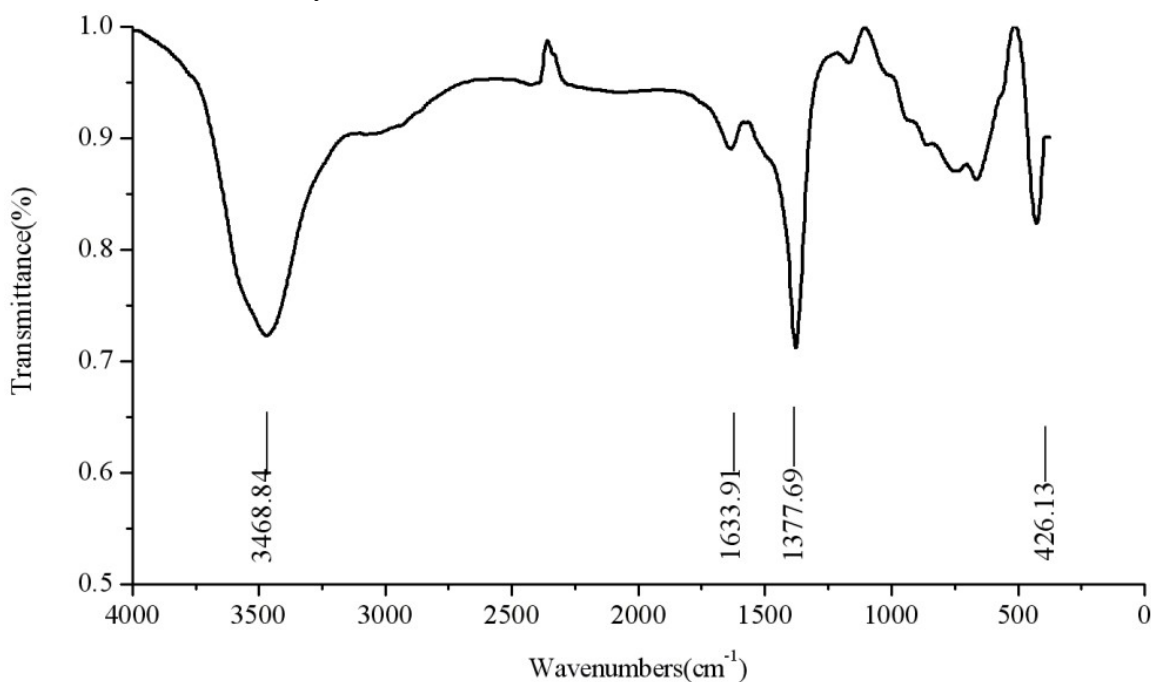


**Fig. 1.** FT-IR spectra of Mg-Al-CO<sub>3</sub> LDH

### X-ray Diffraction Analysis of the Hydrotalcites

The XRD pattern of Mg-Al-CO<sub>3</sub> LDH is shown in Fig. 2. The pattern has the typical peaks of Mg-Al-CO<sub>3</sub> LDH, which can be ascribed to diffraction by planes (003), (006), (009), and (110), especially for the (003) peak ( $2\theta=11.6^\circ$ ). We can also learn from the pattern that the Mg-Al hydrotalcites were regular layered with perfectly crystallized structure, crystallization performance, and thermal stability.

The ideal Mg-Al hydrotalcite colloid should have the features of high amount of charge, well-proportioned distribution of the grain size, and a relatively small average particle size. All these attributes are affected by the experimental conditions, such as pH, the molar ratio of the Mg-Al in the initial reactants, reaction time, the time and temperature of the peptization, and so on. The nature of the particles and their charge can affect the retention directly and determines the effect of its flame retardant. Potential uses of hydrotalcites as a flame-retardant material in flame-retardant paper can benefit from an analysis of the distribution of the particle size, the nature of the charge, and the crystal form.

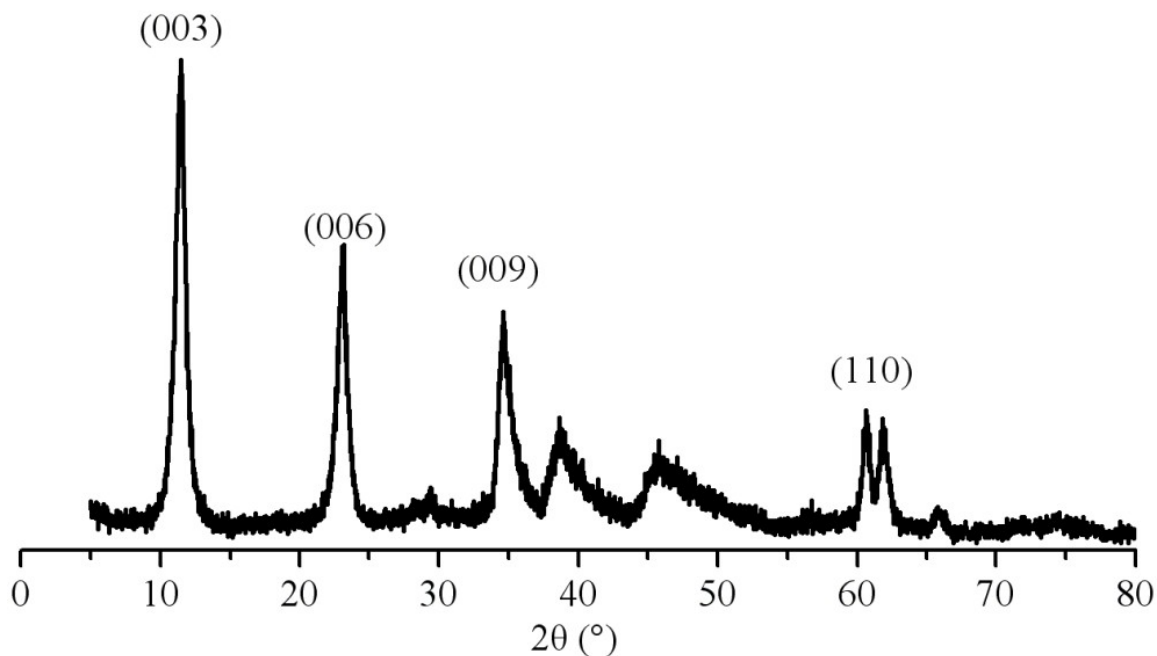
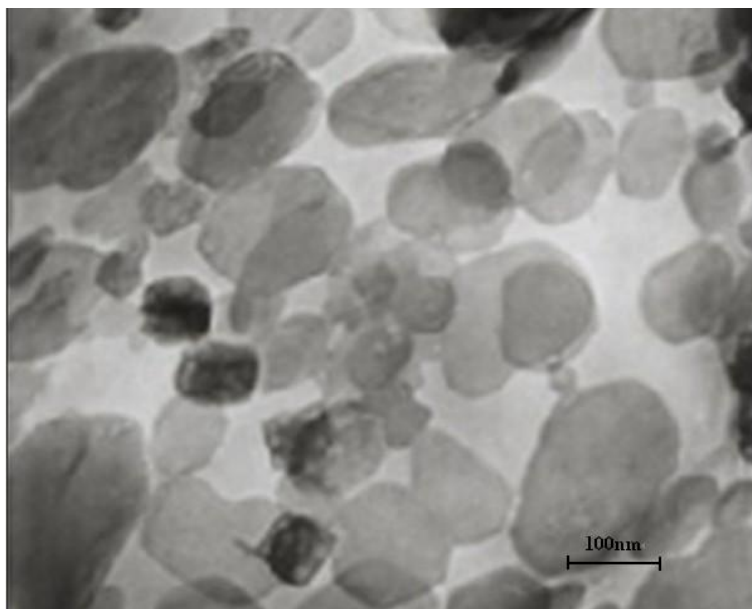


Fig. 2. XRD patterns of Mg-Al-CO<sub>3</sub> LDH

### TEM and SEM Observations of Hydrotalcite Particles

A TEM image (Magnification is 70,000) of Mg-Al hydrotalcites colloidal is shown in Fig. 3, and an SEM image is shown in Fig. 4. It is evident that the colloidal particles of the synthetic hydrotalcites presented a layered structure in which the largest diameter was only 130 nm, and the average particle size was only about 118nm, but the thickness was only a few nanometers. A sheet stacking structure was apparent in most particles, most sheets were of hexagonal and octahedral structure, and a crystalline state was preferred. The most prevalent crystal shape was hexagonal. A minority of the crystals was irregular, and such occurrences may have been caused by crystal defects.



**Fig. 3.** TEM image of Mg-Al-CO<sub>3</sub> LDH

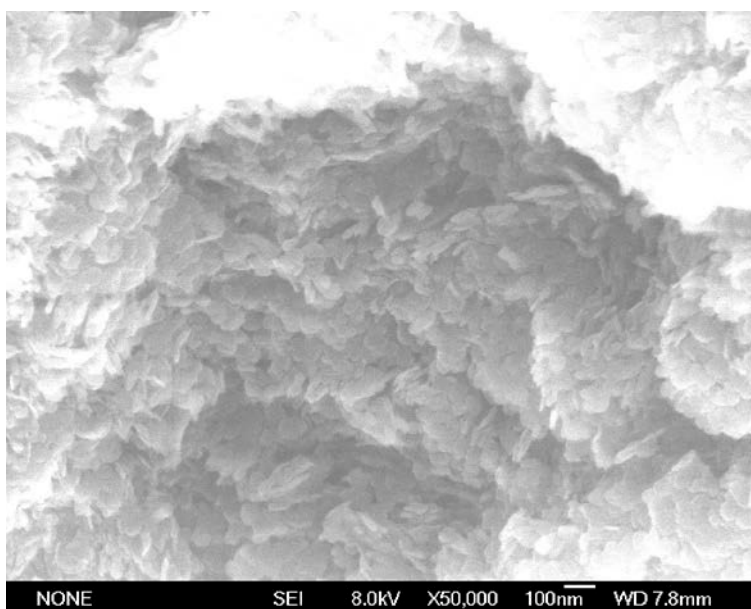


**Fig. 4.** SEM image of Mg-Al-CO<sub>3</sub> LDH

### TG-DTA Analysis of the Hydrotalcites

The TG-DTA curve of Mg-Al LDH is shown in Fig. 5. As can be seen in Fig. 5, Mg-Al LDH exhibits two mass loss steps with increasing temperature. The first one at 50 to 300°C corresponds to the removal of interlayer water, whilst the second one at 300 to 500°C corresponds to dehydroxylation of the layers, loss of interlayer carbonate ions, and breakdown of the layer structure. There were two endothermic peaks on the DTA curve. The obvious endotherm at 209.4°C resulted from the removal of interlayer water and absorption of a large amount of heat. The second peak at 350.4°C resulted from dehydroxylation of the layers and loss of interlayer carbonate ions.

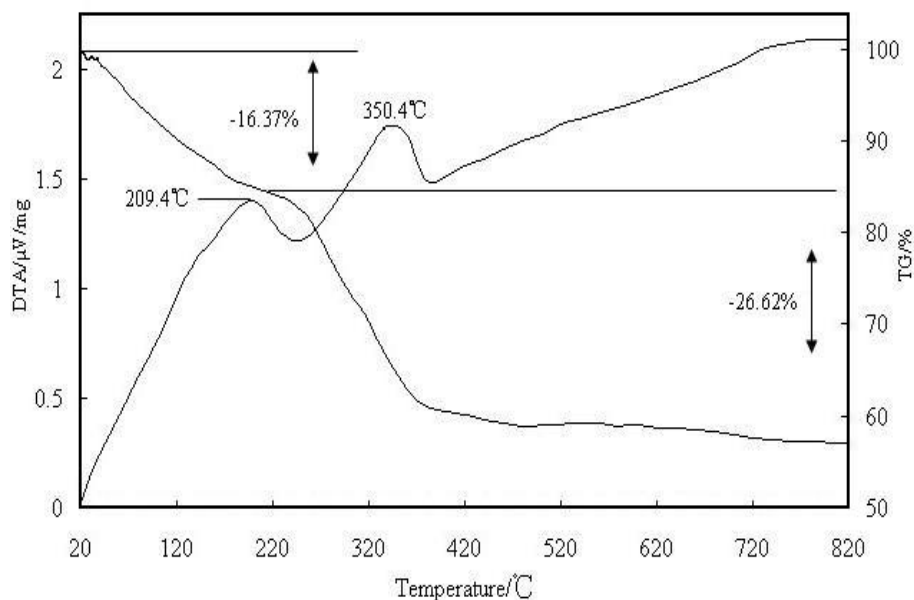


Fig. 5. TG-DTA curve of Mg-Al-CO<sub>3</sub> LDH

### SEM Analysis of Flame-Retardant Paper

An SEM image of paper without Mg-Al LDH is shown in Fig. 6, where it is evident that there were many gaps between fibers. Figure 7 shows the SEM image of flame-retardant paper in which the dosage of Mg-Al LDH was 20wt%. As can be seen in the images, Mg-Al LDH filled the gaps between fibers and adsorbed on fibers firmly. The distribution was even. This good adhesion was attributed to the fact that Mg-Al LDH with high positive charge density can be firmly adsorbed on the fibers.

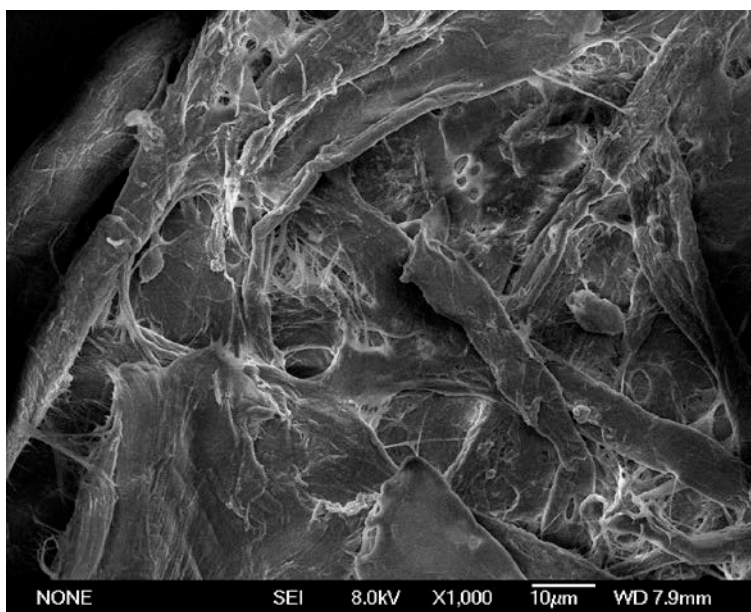


Fig. 6. SEM image of paper without Mg-Al-CO<sub>3</sub> LDH

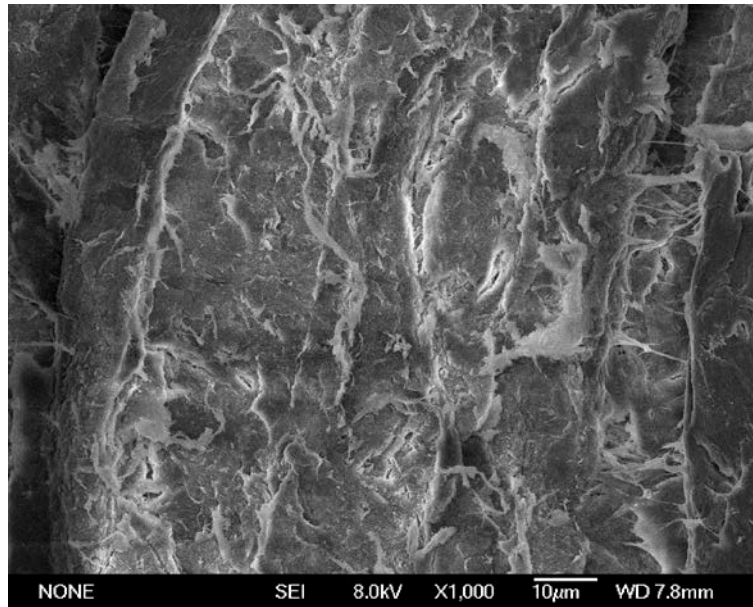


Fig. 7. SEM image of paper with 20wt% Mg-Al-CO<sub>3</sub> LDH

### The Properties of Flame-Retardant Paper

Figures 8 and 9 show the effect of Mg-Al-CO<sub>3</sub> LDH on tensile index and burst index of flame-retardant paper. The tensile index and burst index of flame-retardant paper at first increased and then decreased dramatically with increasing percentage of Mg-Al LDH in the paper. These effects are attributed to the fact that the Mg-Al LDH increased the retention of fines, and then the junctions between fines were increased.

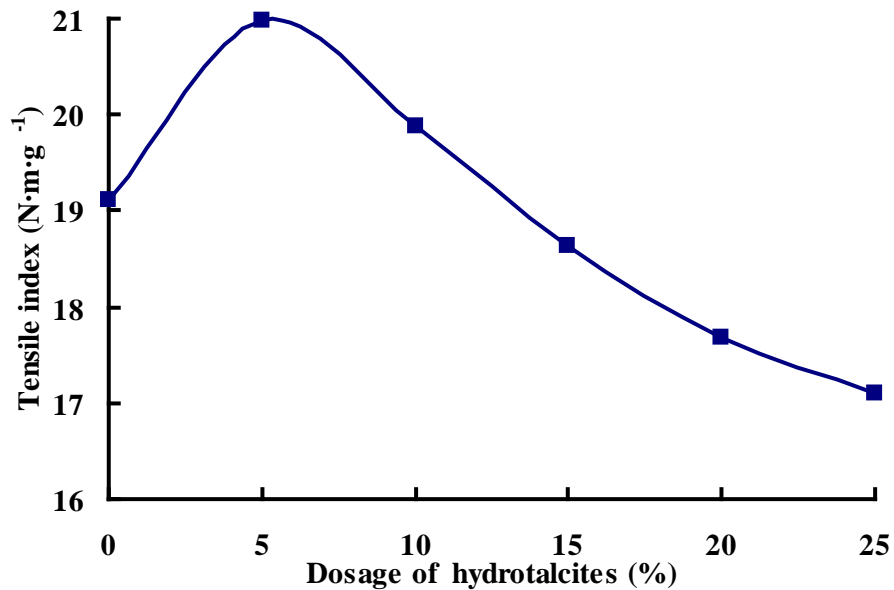


Fig. 8. Effect of dosage of Mg-Al-CO<sub>3</sub> LDH on tensile index of flame-retardant paper



However, when the dosage of Mg-Al-CO<sub>3</sub> LDH was more than 10 percent, the tensile index and burst index were decreased with increasing Mg-Al-CO<sub>3</sub> LDH. These decreases were mainly because the hydrotalcites affected the binding force between the tiny fibers and affected the strength index adversely; it should be noted that the dosage of hydrotalcites was more than the standard filler dosage.

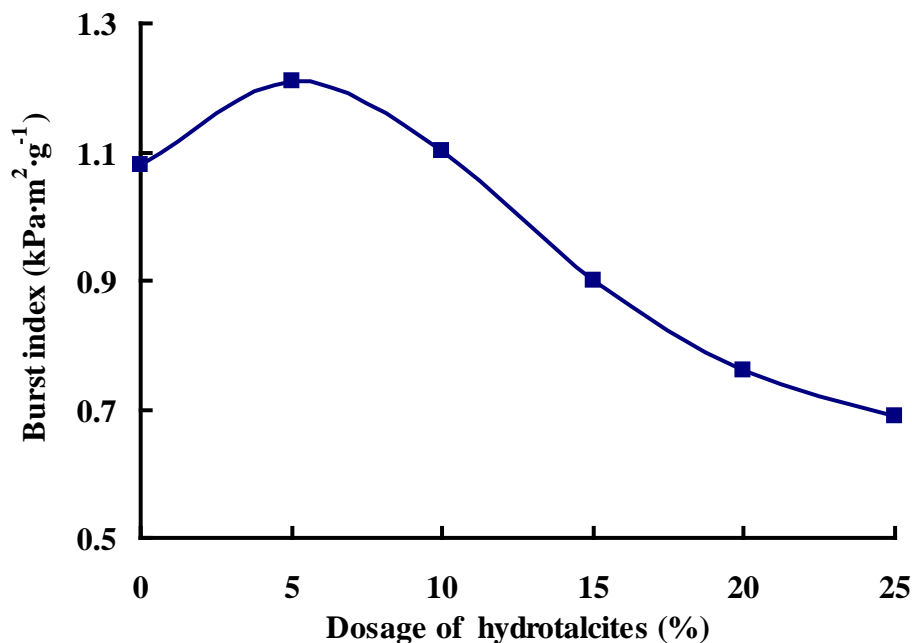


Fig. 9. Effect of dosage of Mg-Al-CO<sub>3</sub> LDH on burst index of flame-retardant paper

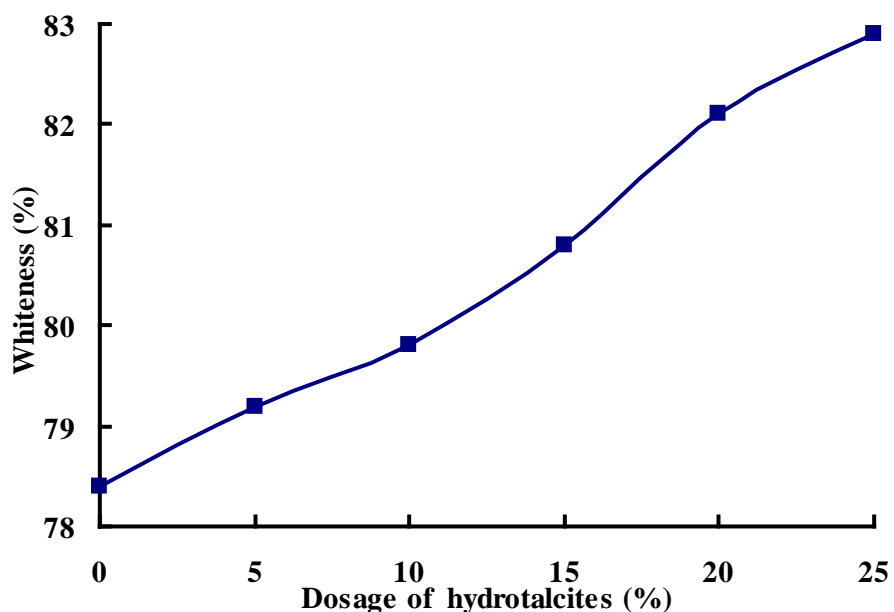


Fig. 10. Effect of dosage of Mg-Al-CO<sub>3</sub> LDH on whiteness of flame-retardant paper

As can be seen in Fig. 10, the whiteness of flame-retardant paper increased with increasing Mg-Al- $\text{CO}_3$  LDH. The whiteness of flame-retardant paper increased by 82.1% when the dosage of LDH was 20wt%; thus, hydrotalcites with high whiteness can improve the whiteness of paper as fillers.

The oxygen index is the lowest oxygen concentration at which a sample can burn in a mixed flow of oxygen and nitrogen gases under the conditions specified. It is defined by the percentage of share of oxygen in the mixed gas.

The paper could not be burnt in air having an oxygen content of 21%, but we prescribe that the oxygen index should be higher than 25%, taking the airflow into account. The flame-retardant paper is preferable, and the oxygen index can be up to 25%. As shown in Fig. 11, the curve oxygen index increased gradually with increasing dosage of hydrotalcites. When the dosage of hydrotalcites was more than 20%, the curve changed slowly. When the dosage of hydrotalcites was 20wt%, the oxygen index reached 25%, indicating that a very good flame-retardant effect can be achieved.

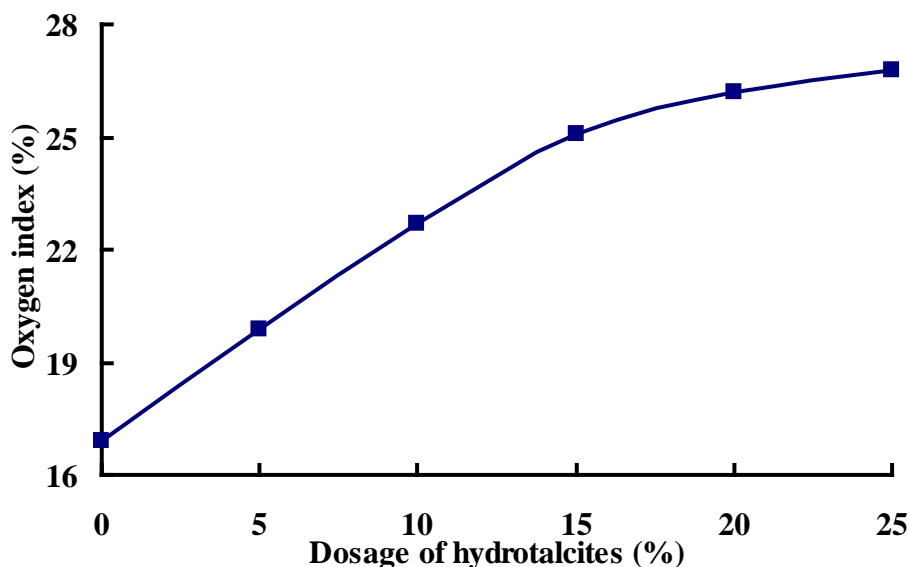


Fig. 11. Effects of dosage of Mg-Al- $\text{CO}_3$  LDH on oxygen index

## CONCLUSIONS

1. Mg-Al hydrotalcites were observed to be layered hexagonal nanoparticles having well developed crystallized structure.
2. Mg-Al hydrotalcites with high positive charge could be adsorbed in the fiber by electrostatic charge attraction in the process of papermaking. They also can perform a role in retention and drainage.
3. Mg-Al hydrotalcites were found to be thermally stable. The thermal decomposition process of Mg-Al LDH included two steps, the removal of interlayer water, and dehydroxylation of the layers, with loss of interlayer carbonate ions.

4. Mg-Al Hydrotalcites adversely affected the physical strength of flame-retardant paper when the content of LDH was more than 10wt%. They also can play the role of filling and whitening. When the dosage of LDH was 20wt%, the whiteness of flame-retardant paper was 82.1%, which was 4.7% higher than the paper without LDH.
5. Mg-Al hydrotalcites were effective paper flame retardants. The oxygen index of the flame-retardant paper was above 25% when the content of Mg-Al hydrotalcites was 20wt%.

## REFERENCES CITED

- Guo, X. (2006). "Production of flame-retardant paper," *Paper and Paper Making* 16(6), 20-23.
- Abbott, C., and Chalabi, R. (1975). *Fire Safety of Combustible Materials*, Edinburgh Oct, 296-299.
- Routley, A. F. (1975). *Fire Safety of Combustible Materials*, Edinburgh. Oct, 1.
- Cavani, F., Trifiro., Vaccari, A. (1991). "Hydrotalcite-type anionic clays: Preparation, properties and applications," *Catalysts Today* 11(2), 173-301.
- Ren, Q., Chen, W., and Liu, B. (2003). "Effect of aluminum resources on flame-retardant property of the Mg/Al-hydrotalcite flame-retardant materials," *Insulating Materials* (6), 2-3.
- Xu, Q., and Xu, J. (1990). "A study on flame retardance mechanisms of  $\text{Al}_2\text{O}_3 \cdot 3\text{H}_2\text{O}$  and  $\text{Mg}(\text{OH})_2$  in HDPE by thermal analysis," *Polymeric Materials Science and Engineering* 6(2), 63-66.
- Shi, L., Li, D., Li, S., Wang, J., Evans, D. G., and Duan, X. (2005). "Structure, flame retarding and smoke suppressing properties of Zn-Mg-Al- $\text{CO}_3$  layered double hydroxides," *Chinese Science Bulletin* 50(11), 1101-1104.

Article submitted: November 23, 2011; Peer review completed: December 19, 2011;  
Revised version received: December 23, 2011; Accepted: January 14, 2012; Published:  
January 17, 2012.